Scientific Journal of Impact Factor (SJIF): 4.72

e-ISSN : 2348-4470
p-ISSN : 2348-6406

International Journal of Advance Engineering and Research Development

National Conference On Nanomaterials, (NCN-2017)

Volume 4, Special Issue 6, Dec.-2017 (UGC Approved)

Luminescence and Structural Properties on Sm^{3+} doped KBr single crystals

D.Roobanguru[1*], S.Bangaru[2]

[1*]Ph. D Research Scholar in Physics, Arignar Anna Govt. Arts College, Namakkal.
[2]Associate Professor of Physics, Arignar Anna Govt. Arts College, Namakkal.

Abstract:- *Single crystals of Sm^{3+} doped KBr were grown by vertical Bridgemann Stockbarger technique. The grown crystal were subjected to the characterization such as Energy Dispersive X-Ray Analysis (EDAX), Fourier Transform Infrared (FTIR), Powder X-ray Diffraction Pattern (PXRD), Scanning Electron Microscopy (SEM), Laser Raman Scattering and Electron Paramagnetic Resonance (EPR) studies. The Laser Raman Scattering and EPR studies on KBr:Sm^{3+} crystals irradiated with γ-rays is reported. PXRD analysis confirms that the crystals belongs to the cubic system with space group of Fm3m. The lattice parameters are given as follows a=b=c=6.596 Å and α=β=γ=90°. The estimated average crystallite size is found to be 4.26μm by using Debye Scherrer's formula. SEM image found to be the particles are irregular lumps to nearly spherical geometry with rounded corners with various sizes from few microns to 5 microns and also cluster is found. The presents of various functional groups was confirmed by using FTIR spectral analysis. EDAX confirm the elements present in the KBr:Sm^{3+} crystals.*

Key words: *KBr, Sm^{3+}, PXRD, EPR, SEM*

1. Introduction

KBr (pure as well as doped with suitable impurities) is probably the most extensively studied of the alkali halides [1–3]. Recent years more efforts have been made for the development of rare earth ions activated luminescent materials for their wide range of potential application in optoelectronic devices, temperature sensors, solid state lighting, optical communication system and luminescent probes [4-9]. Samarium is an active ion for different inorganic host lattice and act as a powerful emitting centre due to its energy level structure and high luminescence efficiency [10]. The large ionic radius of potassium ions permits incorporation of a large number of cationic impurities. The sites of dopants determined by their ionic radii. The radii of Sm^{3+} are 0.958. Most of the work has been done in samarium doped materials as powder and glasses [11-13]. In the present work Sm^{3+} doped KBr crystals has been grown by Bridgeman Stockbarger technique and the grown crystals were characterized by Fourier Transform Infrared (FTIR), X-Ray Diffraction method(XRD), Scanning Electron Microscopy(SEM), Electron Paramagnetic Resonance(EPR).

2. Experimental

Single crystals of Samarium doped KBr (99.99% purity) were grown using Bridgemann Stockbarger technique. Samarium was added in the form of Samarium fluoride (Aldrich 99.99% purity). The crystal grown with three different impurity concentrations 1%, 3% and 5% by weight. The results due to three concentrations were similar except high luminescence yield for crystals with a high concentration. Hence only the results pertaining to Samarium concentration of 5% by weight are presented and discussed. All the measurements were performed at room temperature. Laser Raman Scattering Spectrum were taken using Reinsaaw Invia spectrometer with red laser. X-ray diffraction spectrum of the prepared sample by using (Rigaku) X-ray diffractometer (CuK_α, λ=1.5443Å) at the rate of 2°/min and the variation of 2θ is from 10° to 90°. The morphologies of the samples were inspected using Scanning Electron Microscopy SEM-*JEOL-JSM 5610LV* model. EPR spectrum were recorded using a EPR spectrometer at microwave frequency (9–10 GHz) at room temperature with a magnetic field modulation of 100 KHz to obtained first derivative EPR signal.

3. Laser Raman Scattering

We have used red laser as the excitation wavelength to record Raman spectrum. The Raman spectrum obtained at room temperature using the excitation wavelength λ_L= 785nm is shown in **Fig.1**. It composed of three main peaks at 107Cm^{-1}, 123Cm^{-1} and 139Cm^{-1}. The Raman lines which appear in the range below 200Cm^{-1} are the well known Raman line induced by F-centres in KBr as per the reported work [14]. This exciting laser line is convenient since its wavelength is just located on the wavelength of F-band. Then the Raman spectrum due to F-centres created by γ-ray irradiation does not hide the one induced by V centres.

The Raman spectrum obtained is very weak and is shown in **Fig.1**. Several peaks are observed and obviously some of them are due to F-centres as evidenced by **Fig.1** of a γ-ray irradiated crystal containing only strong F-centres. In the previously reported work [15], Raman spectral lines observed higher than 164cm^{-1} is due to second order Raman spectrum of pure KBr crystal and combination frequency of F-centre modes.

4. Energy Dispersive X-ray Analysis (EDAX)

Fig.2 shows the EDAX spectrum of KBr:Sm^{3+} crystals. From the EDAX analysis, it is confirmed that K, Br, and Sm were present in the finally grown crystal and the percentage of contained elements are shown in **table.I**. From the table, it is clear that there is slight fluctuation in the atomic percent values. This may be due to the small region of samples has been taken for recording the EDAX spectrum. Line trace Sm ion in EDAX evidences that the Sm ion is present in the crystal.

5. Fourier Transform Infrared spectrum

FTIR is the unique tool to identify the functional groups and frequency of vibration between bonds with atoms in the crystal lattice. **Fig.3** shows the FTIR spectrum of KBr:Sm^{3+} crystals in the middle infrared region 4000-400 Cm^{-1}. The bands between 2300-4000 Cm^{-1} are due to OH vibrations of water groups. The appearance of the band related to the stretching vibrations of OH groups at 3403 Cm^{-1}, 2373 Cm^{-1} and C=O groups at 1649 Cm^{-1} in the IR spectrum resulting from the absorption of atmospheric moisture [16]. The high vibration frequency of OH group will increase the non-radiative relaxation and hence decrease the luminescence efficiency. The weak and short bands at 662 Cm^{-1} are due to vibrations of samarium cations at their network sites.

6. Powder X-Ray Diffraction (PXRD)

Fig.4 shows the powder X-ray diffraction pattern of KBr:Sm^{3+} crystals. It is observed that all the observed diffraction peak of the grown crystal are in accordance well with the standard data of KBr (JCPDS No. 04-0531)[17]. They can be indexed to pure cubic structure of KBr with space group of Fm3m. The lattice parameters are given as follows a=b=c=6.596 Å and α=β=γ=90°. No extra phase can be observed indicating those dopants are well incorporated into the host lattice. So the grown sample obtained in a single phase and that doping with the small amount of Sm^{3+} will not induce any impurity phase. The grown crystal are good crystalline nature with strongest intensity peak at 2θ=27.1. The average crystallite size of the grown crystal was calculated using Scherrer's formula $D=k\lambda/\beta\cos\theta$, Where k is the dimensionless shape factor, has a typical value of about 0.9, λ is the X-ray wavelength, θ is the diffraction angle of high intensity peak and β is the full width half maximum of high intensity peak[18]. The strongest peak due to the lattice plane (200) at 2θ=27.1 was used to calculate the average crystallite size of KBr:Sm^{3+} crystals. The estimated average crystallite size is about 4.26nm.

7. Scanning Electron Microscopy (SEM)

SEM image of 3000 magnification in **Fig.5** shows an average particle size is around 5μm with spherical shape particles with agglomerations. The micrograph exhibit particles of irregular lumps to nearly spherical geometry with rounded corners with smooth grain interfaces. Normally, the particle size varies according to their doping elements. Depending upon the nature of doping elements, the particle size varies from smaller sizes to agglomerated particles as clusters. The grown material melt at high temperature at the time of growing would result in the agglomeration of particles. The average particle size is about few microns to 5μm which basically agrees with that estimated from Scherrer equation. According to the reported work [19], the micron size of magnified images indicates that the particle size is suitable for dosimetry applications.

8. Electron Paramagnetic Resonance

EPR spectrum recorded with X-band microwave frequency at room temperature of KBr: Sm^{3+} crystal were shown in **Fig.6**. The most commonly used and commercially available frequency is 9 GHz (X-band). EPR spectrum are readily obtained (at room temperature) only from the f^5 configuration of Sm^{3+}, with its $^6H_{5/2}$ ground state. The sublevels of this state are degenerate in the absence of a crystal field (in a free Sm^{3+} ion). The application of a magnetic field removes the degeneracy and transitions can occur on irradiation with microwave radiation subject to the usual selection rule of $\Delta M_J = \pm 1$. If two or more unpaired electrons are present, so that the total spin S of the electron system is greater than 1/2, one has to take into account the interaction of the electrons with the electric field generated by the surrounding atoms (i.e. the crystal field or ligand field). This interaction causes a splitting of the more than two fold degenerated ground state of the electron system even in the absence of an external magnetic field (i.e. zero field splitting). This interaction results in a line splitting in the ESR spectrum. In the absence of a zero-field splitting, all transitions occur at the same field (corresponding to a g-value of 2.00), but as the zero field splitting increases, transitions occur at higher and lower fields (corresponding to 'effective' g-values above and below 2). The orbitals (atomic or molecular) have two effects: (1) spin-orbit coupling and (2) orbital magnetic field interaction. These effects explain why g is no longer equal to 2.0023 ($=g_e$) and anisotropic. The anisotropy in g is classified into isotropic (one g-value), axial (two g-values) and rhombic (three g-values). The deviation of the principal g-values from the free electron value of 2.0023 carries information about the orbital angular momentum of the electron, i.e. information concerning the electronic structure of the atom or molecules. If one wants to determine g-values from ESR spectrum, one has to know both the field B_0 and the

microwave frequency and calculated the g-factor by means of using the equation $g = h\nu/\mu B_o$, where h is the Planck's constant and μ is the Bohr magnetron. The two resonance signal obtained for grown crystal at 2792 and 2928 gauss. The calculated g-factor for two signal are 2.23 and 2.16.

9. Conclusion

PXRD showed that the grown crystal is a crystalline compound. SEM image found to be the particles are irregular lumps to nearly spherical geometry with rounded corners with various sizes from few microns to 5 microns and also cluster is found. EDAX and FTIR confirm the elements present in the KBr : Sm^{3+} crystals.

Acknowledgements

The authors great fully acknowledges UGC for providing RGNF and UGC – DAE Consortium for scientific Research, IGCAR, Kalpakkam, India for providing experimental support

References

1. A.A.Braner , A. Halperin, and E.Alexander, Phys. Rev. 108, 932 **(1957).**
2. S.C.Jain,PC Mehendru, J. Phys. C: Solid State. 3, 1491 **(1970).**
3. S.C.Ausin, J.L. Alvarez Rivas. J. Phys. C: Solid State 5, 82 **(1972).**
4. S.J.Dhoble, S.K.Raut, N.S.Dhoble, Int. J. Lumin. Appl. 5, 178 **(2015).**
5. G.Blasse, B.C.Grabmaier (Eds), Luminescent Materials, Spinger-Verlag, Berlin **(1994).**
6. G.Blasse, J. All. Comp. 225, 529 **(1995).**
7. C.R.Ronda, J. Lumin. 49, 72 **(1997).**
8. S.Shionoya, W.M.Li, M.Leskela, Phosphor Hand Book CRC press, Newyork, **(1999).**
9. Y.W.Tan, C.S.Shi, J. Sol. Stat. Chem. 150, 178 **(2000).**
10. M.B.Reddy,C.N.Raju, S.Sailaja, B.V.Rao, B.S.Reddy, J. Lumin. 131, 2503 **(2011).**
11. K.Swapna, S.K. Mahamuda, A.Srinivasa Rao, S.Shakya, T.Sasikala, D.Haranath, G.Vijaya Prakash, Spectro. Act. Part A: Mol. Bio. Spec. 125, 53 **(2014).**
12. A.Agarwal, I.Pal, S.Sanghi, M.P.Aggarwal, Opt. Mater. 32, 339 **(2009)**.
13. Z.Wang, P.Li, Z.Yang, Q.Guo, J. Lumin. 132, 1944 **(2012)**.
14. J.P.Buisson,S.Lefrant, A.Sadoc, Taurel.L, M.Billardon, Phys. Stat. Sol. B. 78, 779 **(1976)**.
15. E.Rzepka, J.L.Doualan, S.Lefrant, L.Taurel, J. Phys. C: Solid Stat. Phys. 15 119 **(1982)**.
16. I.P.Sahu, D.P.Bisen, N. Brahme, LumI. 30, 526 **(2015)** .
17. Swanson, Tatge, Natl. Bur. Stand.(US), Circ. 539, 1 **(1951)**.
18. C.G.Hu, Z.W.Zhang, H.Liu, P.X.Gao, Z.L.Wang, Nanotechnology. 17, 5983 (**2006)**.
19. A.H.Oza, N.S.Dhoble, K.Park, S.J.Dhoble, Lumi. 30, 768 **(2015)** .

FIGURE No.1

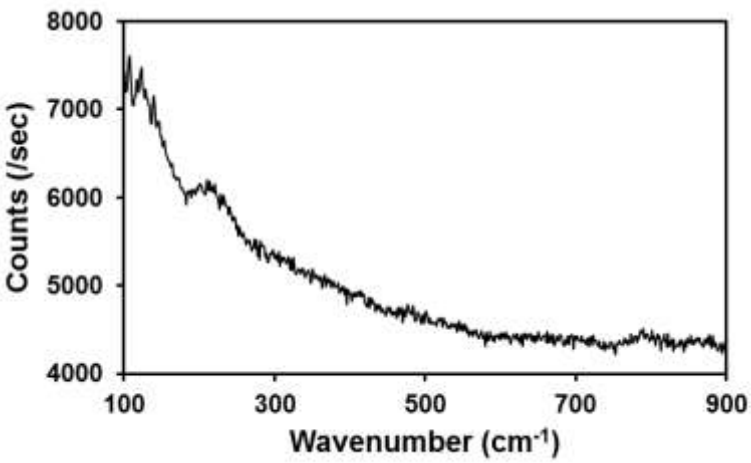

-

Fig.1 Laser Raman Scattering Spectrum KBr : Sm^{3+} Single crystals

FIGURE No.2

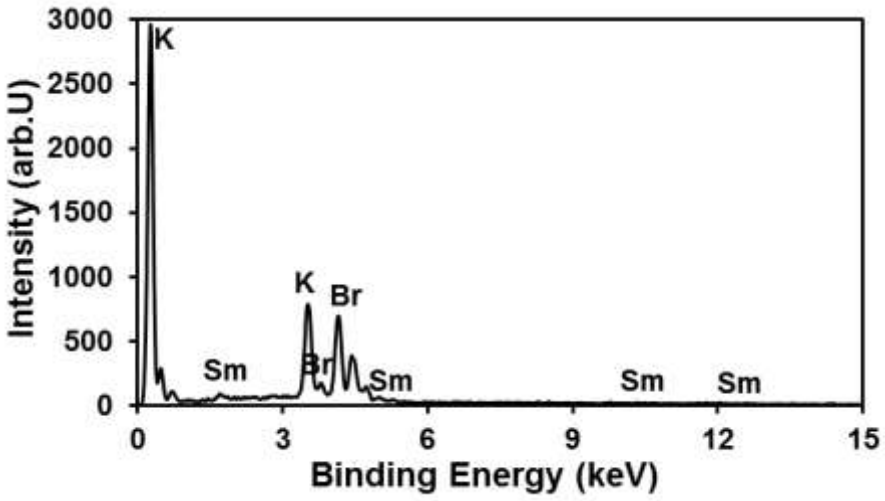

Fig.2 Energy Dispersive X-ray Analysis of KBr :Sm^{3+} single crystals

FIGURE No.3

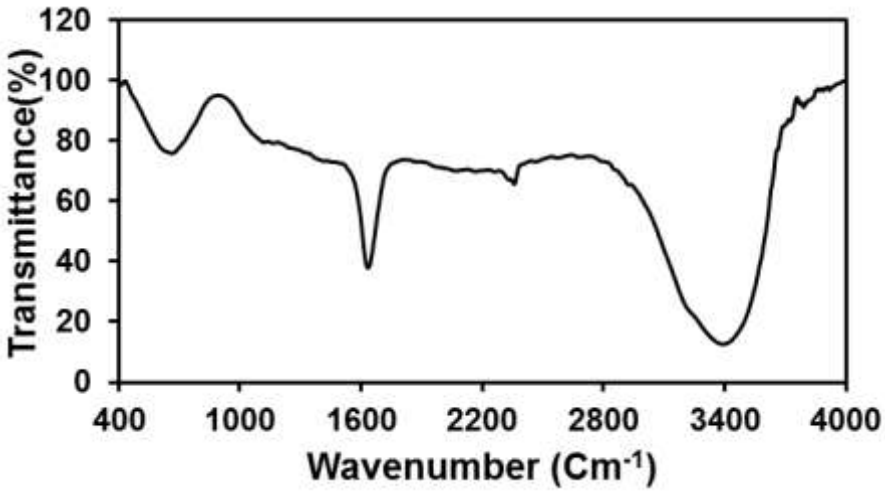

Fig.3 FTIR Spectrum of KBr : Sm^{3+} single crystals

FIGURE No.4

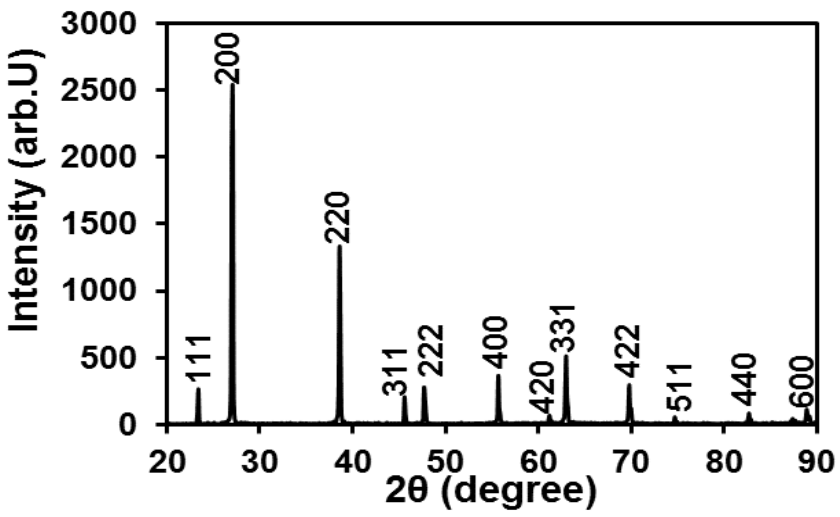

FIGURE No.5

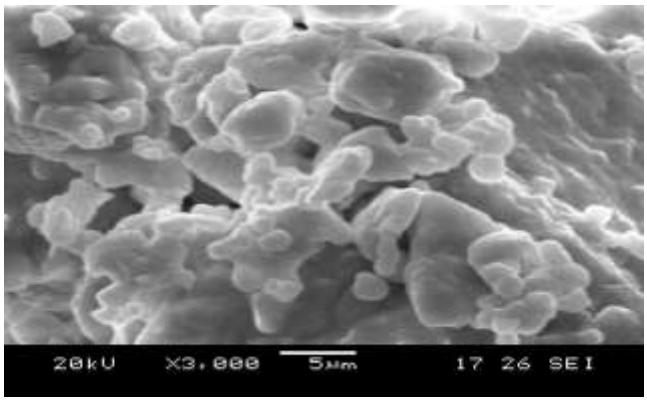

Fig.5 SEM Image of KBr : Sm^{3+} Single crystals

FIGURE No.6

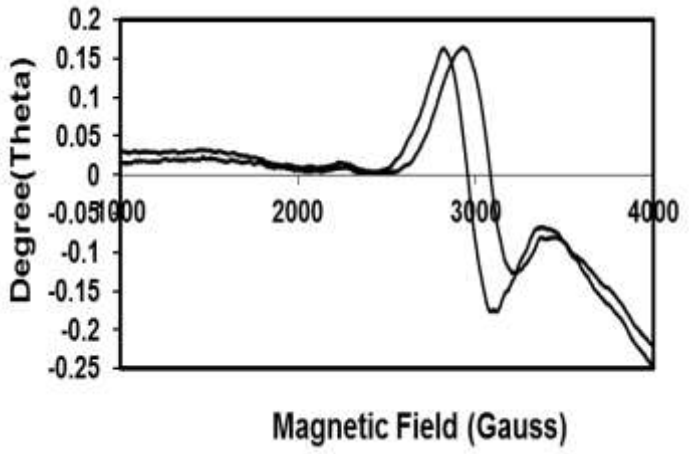

Fig.6 EPR spectrum of KBr : Sm^{3+} Single crystals

TABLE No.I

Table.I Composite element of KBr : Sm^{3+} single crystals

Elements	Intensity (arb.U)	Atomic percentage
K K	1.03	**45.81**
Br L	0.99	**53.64**
Sm L	0.91	**0.55**

